Analytical Biochemistry 421 (2012) 401–410

Contents lists available at SciVerse ScienceDirect

Analytical Biochemistry

journal homepage: www.elsevier.com/locate/yabio

Evaluation of Taylor dispersion injections: Determining kinetic/affinity interaction constants and diffusion coefficients in label-free biosensing

John G. Quinn *

FLIR/ICx Nomadics, Oklahoma City, OK 73104, USA

ARTICLE INFO

Article history:
Received 12 July 2011
Received in revised form 14 October 2011
Accepted 21 November 2011
Available online 1 December 2011

Keywords:
Taylor dispersion
Kinetic analysis
Diffusion coefficient
High-throughput screening
Label-free biosensing
Surface plasmon resonance

ABSTRACT

In label-free biomolecular interaction analysis, a standard injection provides an injection of uniform analyte concentration. An alternative approach exploiting Taylor dispersion produces a continuous analyte titration allowing a full analyte dose response to be recorded in a single injection. The enhanced biophysical characterization that is possible with this new technique is demonstrated using a commercially available surface plasmon resonance-based biosensor. A kinetic interaction model was fitted locally to Taylor dispersion curves for estimation of the analyte diffusion coefficient in addition to affinity/kinetic constants. Statistical confidence in the measured parameters from a single Taylor dispersion injection was comparable to that obtained for global analysis of multiple standard injections. The affinity constants for multisite interactions were resolved with acceptable confidence limits. Importantly, a single analyte injection could be treated as a high-resolution real-time affinity isotherm and was demonstrated using the complex two-site interaction of warfarin with human serum albumin. In all three model interactions tested, the kinetic/affinity constants compared favorably with those obtained from standard kinetic analysis and the estimates of analyte diffusion coefficients were in good agreement with the expected values.

The majority of published kinetic analyses in label-free biosensing have relied on fitting a 1:1 pseudo-first-order interaction model to a series of overlaid binding response curves recorded from fixed concentration injections (FCIs).[1,2] Resolution of multisite binding by FCIs is challenging because it is mathematically difficult to resolve the sum of two superimposed decaying exponentials [1,2]. For example, in fragment screening, many compounds exhibit nonspecific binding [3,4] that greatly exceeds the specific binding response where both binding components overlap in time. However, an affinity isotherm can overcome this superimposition of binding components by providing an analyte titration. Standard affinity analysis requires sequential injection of analyte concentrations over the ligand-coated surface where the contact time for each concentration is sufficient to reach equilibrium. A multisite affinity model is fitted, providing estimates of the affinity constant for the specific binding site [5,6]. The run time for higher affinity interactions is often prohibitive because each injection may require in excess of 1 h to reach equilibrium. Therefore, the increased resolving power of the technique must be balanced against the increased run time. For example, in fragment screening, the number of analyte concentrations required to define the isotherm is often reduced to six or less. Although a less defined isotherm provides less reliable affinity analysis, the results have proven to be adequate in many cases [7]. The resolving power of this steady-state method is a consequence of titrating the analyte, and it was envisaged that a rapid means of performing an analyte titration would provide similar advantages but without sacrificing resolution and/or throughput. We introduce Taylor dispersion injection (TDi) to generate a continuous analyte titration that is suitable for both steady-state and kinetic analyses. Using simple expressions the analyte titration was defined as a function of injection time and substitution into the appropriate binding interaction model enabled direct fitting to the TDi binding response curves. We demonstrate the TDi-based assay format using the following model interactions: scFv binding receptor, furosemide binding carbonic anhydrase II, and finally warfarin binding human serum albumin (HSA).

* Fax: +1 405 235 8608.
E-mail address: john.quinn@icxt.com

[1] This article is the second in a series of two. The following is the first article: J. G. Quinn, Modeling Taylor dispersion injections: Determination of kinetic/affinity interaction constants and diffusion coefficients in label-free biosensing, Anal. Biochem. (accepted for publication).

[2] *Abbreviations used:* FCI, fixed concentration injection; TDi, Taylor dispersion injection; HSA, human serum albumin; SigTDi, sigmoidal Taylor dispersion injection; PulseTDi, pulse Taylor dispersion injection; MTL, mass transport limitation; RU, response units; DMSO, dimethyl sulfoxide; HBS, Hepes-buffered saline; HBS-T, HBS with 0.001% Tween 20; EDTA, ethylenediaminetetraacetic acid; HBS-TE, HBS-T with 3 mM EDTA; rhErbB2/Fc, recombinant human epidermal growth factor receptor 2/crystallizable fragment; scFv, single chain variable fragment; CF, correction factor; SE, standard error; SD, standard deviation; CV, coefficient of variation; RU, response unit.

0003-2697/$ - see front matter © 2011 Elsevier Inc. All rights reserved.
doi:10.1016/j.ab.2011.11.023

Dispersion theory

Taylor dispersion theory is an absolute method that does not require empirical calibration [8] and has been well established for determination of diffusion coefficients [9]. The theory models the physical dispersion process, thereby accounting for variations in flow rate, viscosity, temperature, and capillary geometry and obviating any need for empirical calibration. In practice, TDi is performed in a similar way to standard FCI but with the addition of a large dead volume upstream of the flow cell. Dispersion theory accurately models the effect of the dead volume (i.e., capillary tube) on the analyte concentration when performed in accordance with a defined set of conditions and limits. Dispersion theory can be included in an affinity interaction model by substituting dispersion terms that specify the analyte concentration as a function of injection time. The modified affinity interaction model can then be fitted to TDi data for estimation of interaction constants.

Briefly, tracer dispersion in a flow-through capillary was initially described by Taylor [8] and is illustrated in Fig. 1. An initial sample volume (V_i) containing analyte is injected into a long narrow capillary (Fig. 1A). The analyte concentration is initially uniform but gradually evolves into a sigmoidal gradient profile due to the combined action of analyte diffusion and convective laminar flow (Fig. 1B). Low-molecular-weight molecules diffuse more rapidly than larger molecules and tend to negate convective dispersion more effectively, thereby generating a sigmoidal gradient with increased slope. The analyte enters the flow cell as an increasing analyte concentration gradient where the inflection point of the sigmoidal profile (SigTDi) defines the residence time (τ). This residence time can also be defined as the ratio of the capillary volume to the flow rate, assuming that, on average, the analyte is not retarded relative to the convective flow. Additives (e.g., blocking proteins, surfactants) that block nonspecific binding sites on the capillary wall are sometimes required to prevent retardation. V_i should be large enough to exceed τ in order to produce a full sigmoidal dispersion profile. Injecting a small sample volume (<5% capillary tube volume) into the capillary tube followed by analyte-free buffer produces a dispersion peak (PulseTDi) due to dispersion at both tailing and leading sample fronts (Fig. 1C), where the peak maximum defines the residence time. In PulseTDi,

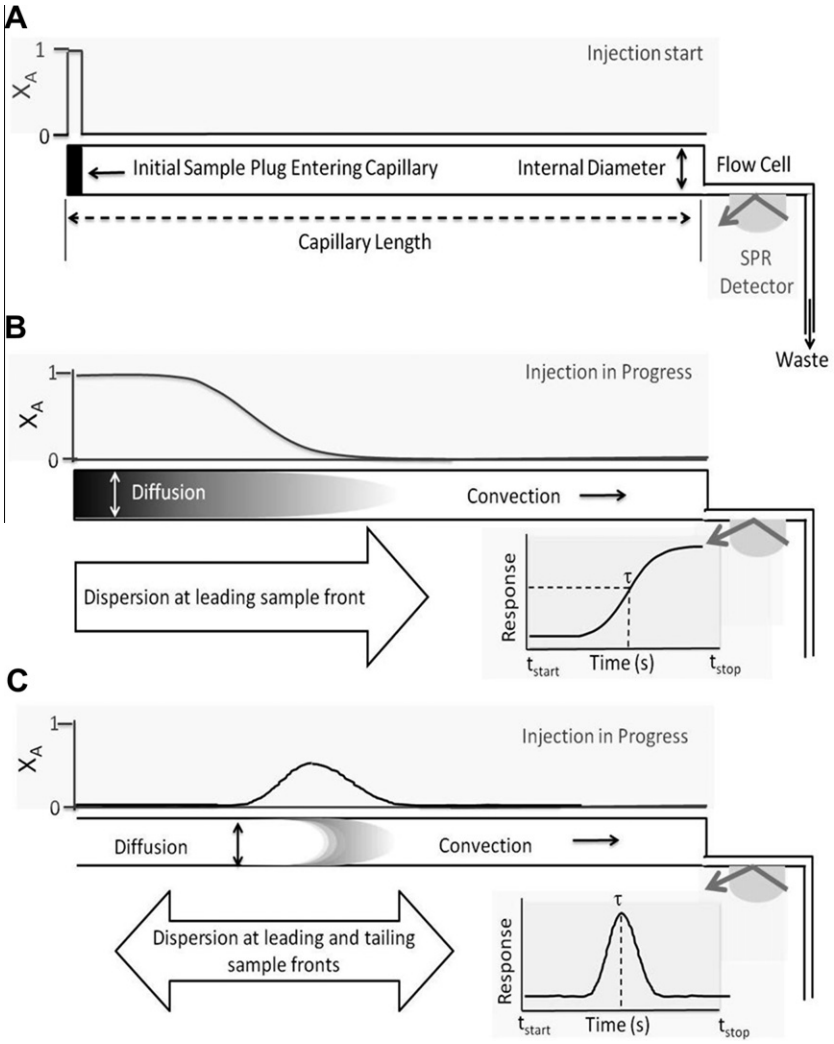

Fig.1. (A) An analyte sample is loaded into a long capillary with a low internal diameter. Pressure-driven flow causes the liquid to exit the capillary into a flow cell that houses the sensing regions. The mole fraction of analyte (X_A) relative to the loaded analyte concentration, C_i, is uniform before migration through the capillary. (B) Continued delivery of sample into the capillary causes the leading analyte front to mix with the buffer occupying the capillary. The relative mole fraction in the flow cell assumes a sigmoidal profile in the flow cell as the injection progresses. (C) In a second case, the initial sample volume migrates through the capillary on continued supply of analyte-free buffer, thereby causing mixing at both the leading and tailing sample fronts. A Gaussian-shaped analyte gradient forms within the flow cell as the injection progresses, giving a maximum relative mole fraction that is significantly lower than unity.

V_i must represent a small fraction (<5%) of the capillary tube volume. The SensíQ Pioneer is a commercially available biosensing system that incorporates a capillary tube suitable for performing the TDi assay formats demonstrated in this article.

TDi modeling

Taylor's analytical solution [8] describing the analyte concentration distribution for PulseTDi is

$$C(t) = \frac{2C_{in}V_i}{\pi^{3/2}d^2\sqrt{kt}}\exp\left[-\frac{0.25L^2(1-t/\tau)^2}{kt}\right] \quad (1)$$

where

$C(t)$ = analyte concentration at detector (mol m^{-3});
C_{in} = concentration of analyte injected (mol m^{-3});
V_i = sample injection volume (m^3);
d = tubing diameter (m);
τ = mean analyte residence time = L/u (s);
L = length of tube (m);
u = average velocity of fluid (m s^{-1});
k = Taylor–Aris dispersion coefficient (m^2 s^{-1});

$$k = \alpha\frac{u^2d^2}{192D} + D \quad (2)$$

D = analyte diffusion coefficient (m^2 s^{-1});
α = correction factor.

We include a correction factor (α) to compensate for any departures from theory. In practice all capillary tubes tested returned $\alpha \cong 1.0$, indicating that Taylor's theory does provide an absolute method. Taylor's solution for SigTDi is given by

$$C(t) = \frac{C_{in}}{2}\left[1 - \operatorname{erf}\frac{1-t/\tau}{2\sqrt{\frac{k}{uL}\frac{t}{\tau}}}\right] \quad (t < \tau) \quad (3)$$

$$C(t) = \frac{C_{in}}{2}\left[1 - \operatorname{erf}\frac{1-t/\tau}{2\sqrt{\frac{k}{uL}\frac{t}{\tau}}}\right] \quad (t > \tau) \quad (4)$$

It is possible to compensate for systematic errors such as injection timing offsets while also verifying dispersion parameters for each individual injection by analyzing bulk refractive index dispersions. For example, TDi analysis of a standard bulk refractive index compound, such as sucrose, or analysis of dispersion curves contained in the reference channel response can be included in each assay. In many cases, a solvent dispersion is present due to a mismatch in concentration between the sample buffer and the running buffer and can serve as an internal standard to verify dispersion parameters before fitting the affinity model. The limit flow rates for a given capillary and analyte for application of dispersion theory are defined as follows. The Peclet number (N_{Pe}) is a dimensionless number that is useful in defining the lower flow rate limit to be used for a given analyte with a given capillary [10]:

$$N_{Pe} = (d.u)/D \text{ with limit } > 500 \quad (5)$$

The upper flow rate limit [10] can be defined in terms of dimensionless time (τ'),

$$\text{where } \tau' = D.\tau/(0.5.d)^2 \text{ with limit } > 3.0 \quad (6)$$

The analyte diffusion coefficient can be estimated [11,12] from the expected M_r of the analyte, allowing calculation of N_{Pe} and τ'. These limits can be automatically calculated before running the assay in order to constrain the experimental conditions within the specified limits.

Kinetic interaction model

The two-compartment 1:1 pseudo-first-order kinetic interaction model is composed of two differential equations that describe the change in the concentration of affinity complexes (dR/dt) at the sensing surface and the analyte concentration gradient (dC/dt) as the analyte passes from the bulk liquid through the diffusion boundary layer to the sensing surface [13,14]:

$$\frac{dC}{dt} = (-k_aC(R_{max} - R) + k_dR + k_m(C_{in} - C)) \quad (7)$$

$$\frac{dR}{dt} = k_aC(R_{max} - R) - k_dR \quad (8)$$

where R is the biosensor response (response units, RU), R_{max} is the maximum response expected if all ligand sites are occupied (RU), and C_{in} is the injected analyte concentration (M), which becomes zero when the dissociation phase begins. C is the concentration (M) of the analyte at the sensing surface, k_m is the mass transport constant (RU M^{-1} s^{-1}), k_a is the association rate constant (m^{-1} s^{-1}), and k_d is the dissociation rate constant (s^{-1}). k_m can be estimated accurately from the following equation [15,16] assuming that the dextran hydrogel does not contribute to mass transport limitation (MTL):

$$k_m = 10^9.M_r.1.43.\left[\frac{1-(L_1/L_2)^{2/3}}{1-(L_1/L_2)}\right].\sqrt[3]{\frac{D^2.F}{H^2.W.L_2}} \quad (9)$$

where F is the flow rate (m^3 s^{-1}) and L_1 and L_2 are the lengths (m) of the functionalized surface relative to the start and end of the sensing region, respectively. H is the height (m) and W is the width (m) of the flow cell. The geometry of the flow cell is well defined, allowing these parameters to be held constant. M_r is usually known or, alternatively, it can be estimated from D [8].

The bulk analyte concentration is the injected analyte concentration (C_{in}) and is constant during FCI. However, in TDi the analyte concentration changes as a function of injection time and can be modeled by substituting the appropriate dispersion term for C_{in}. Fitting the above model, therefore, can include k_a, k_d, R_{max}, k_m, and D as fitted parameters. In many cases, MTL is negligible, where $C_{in} = C$, and the two-compartment model reduces to the simple "rapid mixing" model. Any interaction model of interest can be similarly modified; for example, a two-site interaction model can be chosen where the response recorded by the biosensor, $R(t)$, is given by the sum of multiple components as

$$R(t) = AB(t) + AB_2(t) + RI_{analyte}(t) + RI_{solvent}(t) \quad (10)$$

with fitted parameters k_a, k_{a2}, k_d, k_{d2}, R_{max}, R_{max2}, D and $D_{solvent}$.

Two additive sets of Eqs. (7) and (8) are needed to define the formation of AB plus AB_2 where both incorporate a Taylor dispersion term. Each noninteracting dispersed species is included only when present at a high enough concentration to contribute a significant bulk refractive index response. However, the analyte can often be present at very high concentrations, producing a bulk refractive index term ($RI_{analyte}$). $RI_{analyte}$ will vary in time according to the analyte dispersion profile and can be modeled by the appropriate dispersion Eqs. (1)–(4), where $C(t)$ and C_i are replaced by $RI(t)$ and RI_{max}, respectively, and where $RI_{analyte}(t)$ is the bulk analyte dispersion and RI_{max} is the maximum bulk refractive index response of the analyte in the neat sample. The expected bulk refractive index response for a given concentration of analyte can be approximated by the relation 100 RU $\cong$ 1 mg ml^{-1}, but more accurate estimates have been published [17,18]. Dimethyl sulfoxide (DMSO) is sometimes present at slightly different concentrations in the sample buffer relative to the running buffer, forming

a bulk refractive index dispersion defined by the solvent diffusion coefficient ($D_{solvent}$).

Real-time isotherm model

An affinity isotherm for a complex interaction composed of three affinity sites can be expressed as

$$R_{eq} = R_{max1} * C/(K_{D1} + C) + R_{max2} * C/(K_{D2} + C) + R_{max3} * C/K_{D3} + C \quad (11)$$

The equilibrium response (R_{eq}) is the sum of three affinity binding terms, each defined by independent parameter values for the saturation response (R_{max}) and affinity constant (K_D) at each binding site. However, this affinity model cannot be fitted directly to the real-time TDi isotherm and therefore cannot be used to determine *D*. Therefore, we composed an affinity isotherm model that is analogous to Eq. (11) but where R_{eq} was expressed as a function of injection time, $R_{eq}(t)$, allowing the isotherm model to be fitted directly to the TDi curve:

$$R_{eq}(t) = R_{max1} * C(t)/(K_{D1} + C(t)) + R_{max2} * C(t)/(K_{D2} + C(t)) + R_{max3} * C(t)/K_{D3} + C(t) \quad (12)$$

where $C(t)$ is given by Eqs. (1)–(4). Because this isotherm model is complex, it is recommended that two or more TDi curves be used in order to constrain fitted parameters globally for improved performance.

Materials and methods

Instrument, sensor chips, and chemicals

SensíQ Pioneer, sensor chips, and chemical coupling reagents were obtained from FLIR/ICx Nomadics (Oklahoma City, OK, USA, http://www.discoversensiq.com). All analyses were performed at 25 °C unless otherwise stated. All other reagents were obtained from Sigma (St. Louis, MO, USA). The running buffer contained 10 mM Hepes and 150 mM NaCl (pH 7.4) (Hepes-buffered saline, HBS) with 0.001% Tween 20 (HBS-T) and 3 mM ethylenediaminetetraacetic acid (EDTA) (HBS-TE) unless otherwise stated. Five dispersion tubes of varying dimensions were evaluated: tube A with V_t = 509 μl, d = 0.227 mm; tube B with V_t = 500 μl, d = 0.38 mm; tube C with V_t = 512 μl, d = 0.50 mm; tube D with V_t = 52 μl, d = 0.25 mm, and tube E with V_t = 120 μl, d = 0.25 mm. Recombinant human epidermal growth factor receptor 2/crystallizable fragment (rhErbB2/Fc) chimera was purchased from R&D Systems (Minneapolis, MN, USA), and anti-ErbB2 single chain variable fragment (scFv) was a kind donation by a company that wished to remain anonymous.

General TDi analysis

Ethylene tetrafluoroethylene (ETFE) and polyether ether ketone (PEEK) tubing was obtained from Upchurch Scientific (Oak Harbor, WA, USA) and cut to the required length to hold approximately 500 μl of liquid when full. The tubing was fitted in the SensíQ Pioneer, connecting the injector valve to the reaction flow cell. The autosampler performed unattended loading of samples contained in a cooled aluminum sample rack. Method programming enabled gradient analyte injections to be performed. Routine purging routines were incorporated into each sample cycle. The system was precleaned with 0.5% sodium hypochlorite and then coated with 0.1% Tyloxapol in water to minimize analyte interactions with the surface of the flow channels. A COOH5 sensor chip was installed in the SensíQ Pioneer system, and the system was primed with HBS-TE. The flow rate was chosen to give a low retention time, allowing Taylor analysis to be conducted at analysis cycle times comparable to a single FCI cycle. The viscosity of HBS was assumed to be 0.94 Cp at 25 °C, and a linear correction factor (CF) for both temperature and viscosity was employed to standardize *D* measurements recorded under nonstandard conditions [12] diffusion coefficient ($D_{solvent}$).

Bulk refractive index TDi for estimation of D

For determination of diffusion coefficients, the concentration of analyte was high enough to produce a significant bulk refractive index response. A series of biomolecule standards was prepared at 10 mg ml^{-1} in HBS-TE running buffer immediately before priming the system into the same buffer to ensure that the bulk refractive index difference between the injected sample and the continuous flow buffer was due entirely to the added biomolecule. The analysis was performed for glycine (M_r = 75), alanine (M_r = 89), β-cyclodextrin (M_r = 1135), vancomycin (M_r = 1485), polyvinyl pyrrolidine (M_r = 1.0 × 10^4), ribonuclease (M_r = 1.37 × 10^4), carbonic anhydrase II (M_r = 3.0 × 10^4), ovalbumin (M_r = 4.5 × 10^4), bovine serum albumin (M_r = 6.6 × 10^4), antibody fragment (M_r = 2.75 × 10^4), antibody (M_r = 1.5 × 10^5), and dextran (M_r = 1.07 × 10^4, 3.7 × 10^4, 5.0 × 10^5).

In PulseTDi, a sample volume of 12 μl was loaded and injected at 50 μl min^{-1} followed by running buffer and allowed to migrate through the capillary tube (tube A) before reaching the sensing regions. The bulk refractive index was recorded where 1 RU was equivalent to 1 μg ml^{-1} analyte. The recorded bulk refractive index response curves were fitted to Eq. (1) using GraphPad Prism (GraphPad Software, La Jolla, CA, USA). In bulk PulseTDi analysis, $C(t)$ was replaced by $RI_{analyte}(t)$ and C_{in} was replaced by RI_{max}. The injected sample volume, volume of the tube, and *D* were fitted locally for each curve while the remaining parameters were held constant. For SigTDi an injection volume of approximately 1.5-fold the capillary tube volume is required in order to produce a complete sigmoidal analyte gradient profile. However, rather than consuming such a large volume of sample we obtain equivalency results by injecting a sample volume of 0.5-fold the tube volume followed uninterrupted by an air bubble (approximately 2 *uL*) and continuous running buffer to a final combined volume of approximately 1.5-fold the capillary tube volume.

Curve fitting

Throughout this article, parameter values are presented where the last significant digit is followed by parentheses containing the standard error (SE) associated with that digit. Curve fitting to kinetic interaction curves was performed using GradFit, a custom simulation and curve-fitting package developed by BioLogic Software (Campbell, Australia, http://www.biologic.com.au). GradFit software uses numerical integration of the binding rate equations to generate simulations and fit interaction models to interaction curves. A scripting interface provided a convenient model-building environment to construct interaction models with or without a mass transport term. Data fitted in GradFit were exported into GraphPad Prism and plotted. Qdat, a customized version of the well-known Scrubber data analysis software from Biologic Software, was employed for double referencing [19] of all data sets, with the exception of the bulk refractive index-based TDi data, which was referenced by simply subtracting the response for a blank buffer sample. The derivative curves in Fig. 5 below (see Results and Discussion) were prepared using Microsoft Excel. The appropriate PulseTDi or SigTDi term was included when fitting all TDi data.

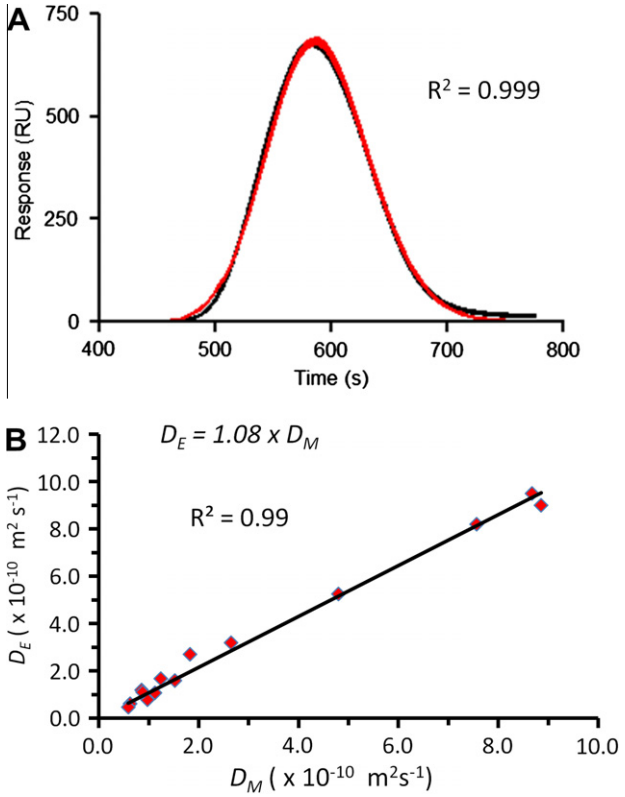

Fig.2. (A) PulseTDi analysis of vancomycin. Vancomycin was diluted to 10 mg ml^{-1} in running buffer and injected through capillary tube A at 50 µl min^{-1} at 25 °C. The recorded bulk refractive index response did not possess a surface binding component. The injection was repeated in quadruplicate, and curves were superimposable. The peak (black curves) was fitted (red curve) with Eq. (1), where the geometry of the capillary tube and flow rate were held constant, allowing accurate estimation of the diffusion coefficient. The volume of sample injected was confirmed by integrating the peak. In each case, the target volume of 12 µl was attained to within 5%. The procedure was repeated for 20 different biomolecules over an M_r range of 75 to 5 × 10^5. (B) The measured diffusion coefficients ($D_{measured}$) were plotted against the expected diffusion coefficients ($D_{expected}$), and a regression line was fitted. (For interpretation of the references to color in this figure legend, the reader is referred to the Web version of this article.)

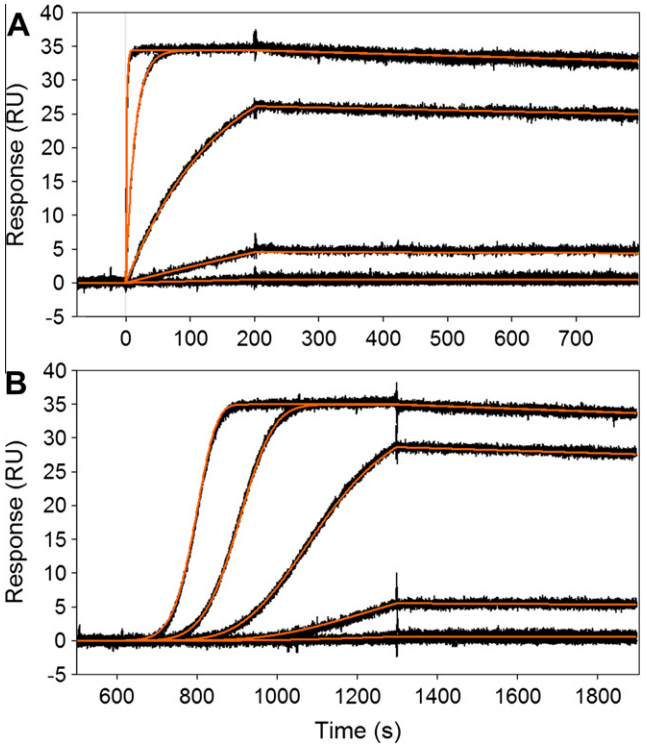

Fig.3. Overlaid binding response profiles for the interaction of scFv with affinity-captured rhErbB2/Fc. The data acquisition rate was 8 Hz, and the SD of the residuals for all fits was less than 0.20 RU. The fitted model (smooth red curves) is superimposed on the experimental curves (rough black curves). (A) FCI analysis. scFv was injected at 50 µl min^{-1}, in duplicate, using serial 10-fold dilutions from 1000 to 0.1 nM. (B) SigTDi analysis. scFv was injected at 50 µl min^{-1}, in triplicate, using serial 10-fold dilutions from 1000 to 0.1 nM. A number of model-fitting variations were evaluated, and the results are given in Table 1. A simple "rapid mixing" model with fitted parameters k_a, k_d, R_{max}, and D is shown.

Antibody fragment–receptor interaction

For the standard FCI format, a sensing chip with a carboxylated dextran-based hydrogel (COOHV) was installed and the biosensor was primed into HBS-TE buffer. Protein G was immobilized onto two sensing channels by standard amine coupling to a mass equivalent to 1200 RU. Each binding interaction cycle was performed as follows. The fusion protein, rhErbB2/Fc, was diluted to 10 nM in running buffer and captured onto the first channel by injecting 50 µl at 25 µl min^{-1}, whereas the second channel was left uncoated and used for double referencing of the data set. scFv diluted in running buffer was then injected over both channels at 50 µl min^{-1}, and dissociation was observed for 10 min. The surface was regenerated with a 60-s exposure of both channels to 20 mM NaOH. This series of three injections was repeated for each cycle.

For SigTDi, the experiments were performed as described for FCI with the following differences. Here, 250 µl of analyte sample was injected at 30 µl min^{-1} through the capillary tube (tube B) prior to contacting the sensing surface. The residence time (τ) is equal to the injected sample volume divided by the flow rate, and the full sample contact time must exceed τ in order for the gradient to exceed the maximum analyte concentration. Therefore, the contact time was chosen such that the total volume injected approached 1.5-fold the capillary volume. Both FCI and TDi assays were performed during the same assay run, over the same sensing surfaces, and using the same reagent preparations in order to minimize experimental variability and enable accurate comparison of the techniques.

Analysis of furosemide–carbonic anhydrase II interactions

Carbonic anhydrase II was immobilized onto a sensing surface by amine coupling. A second sensing surface remained uncoated to provide an accurate reference surface. A mass equivalent to approximately 4500 RU of carbonic anhydrase II was immobilized. Furosemide binding was tested at 25 °C by dissolving the drug directly in HBS-T to 1 mM and then making dilutions of this stock concentration as required. EDTA was excluded from the buffer to maintain the binding activity of the Zn-dependent carbonic anhydrase II. TDi analysis was performed at a flow rate of 100 µl min^{-1} using capillary tube C. A complex binding data set was recorded by allowing the carbonic anhydrase II-coated surface to degrade at 25 °C for 4 days before performing a SigTDi analysis. All TDi injections contained 250 µl of analyte sample.

Affinity ranking

HSA was immobilized by standard amine coupling onto a COOH5 chip surface, giving a loaded mass equivalent to 10 kRU where 1 RU = 1 response units = 1 × 10^{-6} refractive index units and represents a surface mass loading of 1 pg mm^2. Warfarin was prepared as 33-mM stocks in DMSO and then diluted to the neat working concentration in HBS-TE with a final DMSO

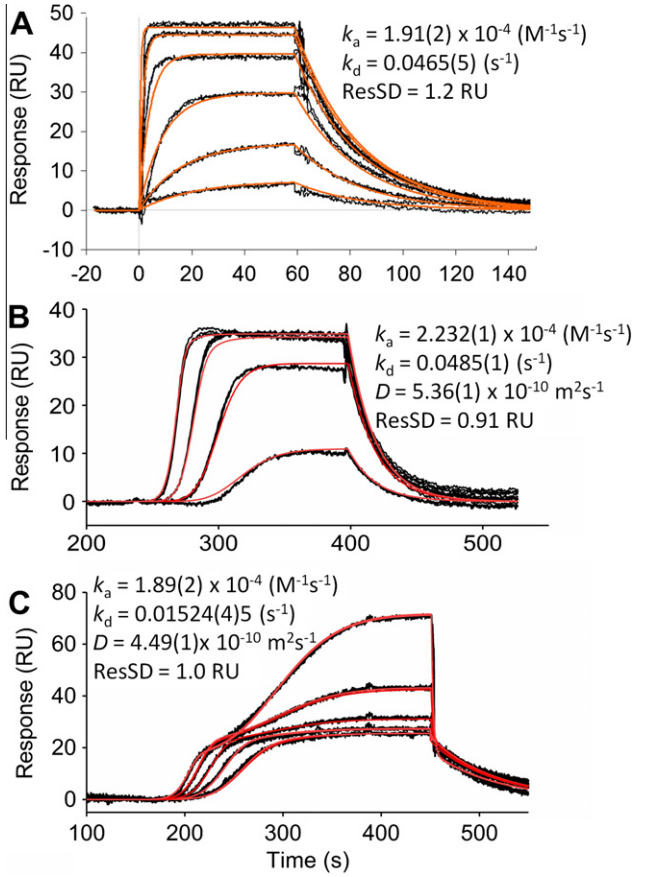

Fig.4. Furosemide–carbonic anhydrase II binding response curves. Each injected concentration was performed in duplicate. (A) FCI analysis. Carbonic anhydrase II was immobilized by amine coupling, and serial 3-fold dilutions of furosemide from 0.46 to 111 μM were injected at 50 μl min^{-1}. A global fit of a simple 1:1 kinetic interaction model was applied (smooth red curves). (B) SigTDi analysis. Carbonic anhydrase II was immobilized by amine coupling, and four serial 10-fold dilutions of furosemide from 1 μM to 1 mM were injected by TDi at 100 μl min^{-1}. A global fit of a simple 1:1 kinetic interaction model was applied (smooth red curves). (C) SigTDi analysis. A carbonic anhydrase II-coated surface was permitted to degrade over several days at 25 °C. Serial 3-fold dilutions were injected from 12 μM to 1 mM at 50 μl min^{-1} by TDi. The analysis was performed at 10 °C to preserve weak nonspecific binding in order to mimic a realistic complex data set. A 2:1 simple interaction model was fitted globally (smooth red curves) where only R_{max2} was allowed local values. Returned parameter values are shown with the SE associated with the last digit in parentheses. (For interpretation of the references to color in this figure legend, the reader is referred to the Web version of this article.)

concentration of 3%. Sample injections of 250 μl were injected at 100 μl min^{-1} through capillary tube A for a contact time of 390 s.

Real-time isotherm

HSA was immobilized by standard amine coupling onto a COOHV chip surface, giving a loaded mass equivalent to 4.5 kRU. The surface was allowed to stabilize for 24 h in order to limit conformational shifting of HSA. Warfarin was prepared as a 33-mM stock in DMSO and then diluted to 1 mM, the neat working concentration, in HBS-TE with a final DMSO concentration of 3%. For PulseTDi, 5 μl of sample was injected at 25 μl min^{-1} into capillary tube D and the injection was terminated after 158 s. This injection was repeated for a series of 12 serial 2-fold dilutions in triplicate. Data were double referenced in Qdat before model fitting. For SigTDi, 60 μl of 1 mM warfarin was injected at 10 μl min^{-1} and terminated after 1040 s. Regeneration was not necessary because warfarin dissociated rapidly from the HSA-coated surface. The buffers contained approximately 3% DMSO, and the resulting bulk

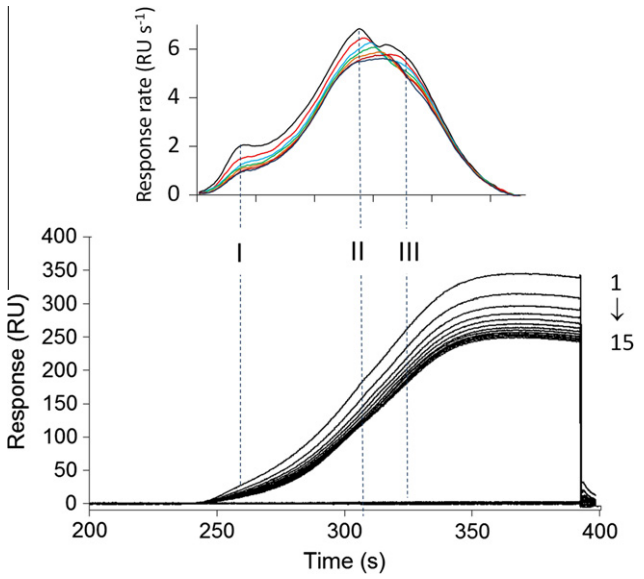

Fig.5. Time progression series of overlaid SigTDi binding response curves for a warfarin–HSA interaction. Here, 250 μl of 3 mM warfarin was injected by TDi over amine-coupled HSA for 15 replicates at 15-min intervals. Inset: Derivative of the first seven binding curves after a 5-point smoothing. Data were recorded at 8 Hz for enhanced resolution of the derivative curve. The derivative curves contain three or more distinct peaks associated with different binding site populations and indicated by the vertical broken lines and Roman numerals.

refractive index offsets were eliminated by conventional double referencing. The presence of DMSO offsets also causes a non-negligible offset in sensitivity between sensing channels that is related to an excluded volume effect. The sensing channels were normalized using bulk refractive index standards to compensate for this effect.

Results and discussion

Bulk refractive index TDi

A series of biomolecules over a wide molecular weight range (M_r = 75 to 5 × 10^5) were analyzed using bulk refractive index PulseTDi analysis. The resulting PulseTDi curves were fitted with Eq. (1) (where $C(t)$ and C_i were replaced by $RI_{analyte}(t)$ and RI_{max}, respectively) for estimation of diffusion coefficients. A set of four superimposed curves for vancomycin are shown in Fig. 2 with the model fitted. The diffusion coefficients for a set of biomolecules were determined by this method, and the measured diffusion coefficients ($D_{measured}$) were compared with the literature values ($D_{expected}$) [12], giving a correlation coefficient of 0.995. In addition, the linear regression analysis gave R^2 = 0.999. This agreement between the TDi curves and theory validates the application of the Taylor dispersion model. The determination of diffusion coefficients by solution-phase Taylor dispersion methods is well known [9], but its use in biosensing provides new possibilities of practical value in routine applications. In particular, D can also be determined as a fitted parameter from the solid-phase binding interaction curves, reducing the amount of analyte sample required and allowing crude analyte samples to be used. Measurement of the diffusion coefficient by either the solution- or solid-phase TDi methods is particularly valuable in confirming the absence of analyte aggregates.

Antibody fragment–receptor interaction

The interaction of scFv with ErbB2-Fc bound to a sensing surface was analyzed by both FCI and TDi, giving the response curves

Table 1
Parameter values returned for global fitting of the simple "rapid mixing" model and the two-compartment model.

Model type	k_a (M^{-1} s^{-1})	k_d (s^{-1})	R_{max} (RU)	D (m^2 s^{-1})	k_m (RU M^{-1} s^{-1})	Concentration (M)
Simple	$7.094(3) \times 10^5$	$7.20(2) \times 10^{-5}$	34.597(7)	Fixed	–	Fixed
Simple	$6.398(1) \times 10^5$	$6.87(2) \times 10^{-5}$	35.018(2)	$8.878(2) \times 10^{-11}$	–	Fixed
Simple	$6.5(2) \times 10^5$	$6.91(2) \times 10^{-5}$	35.012(2)	Fixed	–	1.01 μM
Two-compartment	$7.15(1) \times 10^6$	$8.90(4) \times 10^{-5}$	34.531(4)	Fixed	$1.0(1) \times 10^9$	Fixed
Two-compartment	$6.592(2) \times 10^5$	$6.94(2) \times 10^{-5}$	35.007(2)	$8.859(2) \times 10^{-11}$	Linked to D	Fixed
Two-compartment	$6.517(3) \times 10^5$	$6.92(1) \times 10^{-5}$	35.012(2)	$8.864(1) \times 10^{-11}$	$6.9(2) \times 10^8$	Fixed

Note. The data from Fig. 3 were fitted with a number of interaction models. Parameters that were constrained to known best fit values are indicated by "Fixed." k_m is by definition absent from the Simple model since mass transport of analyte is assumed to be infinitely fast. By representing k_m using Eq. (9) and coupling the fitted parameter D to this expression, it was possible to link the estimation of k_m to estimates of D, as indicated by "Linked to D." The number in parentheses for each parameter value is the SE of the last significant digit.

Table 2
k_a Values returned from local fitting of TDi curves and FCI curves and relative error with respect to the global parameter values.

nM	FCI		TDi	
	k_a (M^{-1} s^{-1}) $\times 10^5$	% Relative error	k_a (M^{-1} s^{-1}) $\times 10^5$	% Relative error
10	8.29(3)	16.86	6.03(1)	5.23
10	6.80(1)	4.14	6.42(1)	0.90
10	–	–	6.30(1)	0.99
100	4.59(2)	35.30	6.277(5)	1.35
100	5.74(3)	19.09	6.426(5)	0.99
100	–	–	6.358(5)	0.08
1000	6.62(1)	6.68	5.899(6)	7.28
1000	8.04(3)	13.34	5.946(6)	6.65
1000	–	–	5.883(6)	5.23

Note. The data from Fig. 3 were fitted with the simple model where k_a, k_d, R_{max}, and D were fitted locally to each curve. k_m was constrained to a constant value. The average SD of the residuals for each local fit was less than 0.2 RU.

in Fig. 3 and the parameter values in Table 1. A global fit of a 1:1 interaction model to FCI data gave kinetic constants that were comparable (<15% variation in any fitted parameter) to those from the TDi model fit, and the average standard deviation (SD) of the residuals was low (~0.2 RU) for both data sets. All replicates were superimposable, and TDi data were comparable in quality to FCI data. The absence of any systematic deviation of the fitted model over such a wide concentration range (four orders of magnitude) implies that the TDi concentration profile conforms to model predictions even at high dilution factors. The fitted TDi model returned $D = 8.878(2) \times 10^{-11}$ m^2 s^{-1} for the scFv analyte, which was within 5% of the expected value [20]. In addition, the fitted k_m from TDi was in excellent agreement with k_m calculated from theory, whereas k_m from FCI was 50% higher. Therefore, TDi returned accurate estimates of k_m, and the correspondence with theory implies that the dextran hydrogel did not contribute significantly to MTL given that this source of MTL is not accounted for in the theory. In general, the TDi method provided higher confidence in the measured parameters, as indicated by lower SEs in estimated parameters.

A particularly useful benefit of TDi is apparent when the data in Fig. 3 are fitted locally. Local model fitting to a single binding curve far from the R_{max} is known to return unreliable results [21]; therefore, such curves were omitted. The difference between TDi and FCI largely concerns determination of k_a, with no significant change in determination of k_d. Fortunately, k_d can be established accurately for single curves that approach R_{max}, a condition that is usually not difficult to achieve. Table 2 shows k_a values returned from local fitting to both data sets and the relative error with respect to the global parameter values. TDi outperformed FCI dramatically, giving a 5-fold lower maximum relative error. The SE returned for each parameter was also significantly lower for TDi, giving estimates that were lower than those from a global fit to FCI data. The estimates of D returned from local fitting were extremely precise, giving a coefficient of variation (CV) of only 0.5%, and the mean for the set of local fits was within 3% of the global value. Therefore, the data strongly suggest that a local fit to a single TDi curve provides kinetic constants that are as robust as those from global fitting to a set of standard FCI curves. The data also demonstrate the value of global model fitting when using standard FCI data.

TDi and mass transport limitation

When characterizing PEGylated antibody fragments, Kubetzko and coworkers [22] determined the active concentration and kinetic interaction constants from separate assays, and dynamic light scattering provided accurate M_r. TDi can potentially perform all three measurements. For example, values of D recovered from a fit of an interaction model to TDi data can be used to estimate M_r from empirical correlations [12], obviating the need for a pure analyte sample at high concentrations as required in techniques such as dynamic light scattering. Experimental conditions can be chosen such that sufficient MTL is present for estimation of the active analyte concentration while also estimating kinetic interaction constants and D from the fitted model. The data in Fig. 3 were recorded on a low MTL surface, and (intuitively) analysis of these data would not be expected to provide accurate estimation of parameters that depend on MTL such as active concentration. Surprisingly, it was possible to obtain good estimates for k_a, k_d, D, k_m, and active concentration from this data set. The degree of MTL can be estimated as follows: $\%MTL = 100 * (k_a * R_{max})/[(k_a * R_{max}) + k_m]$, giving a value of 3.1% for the TDi data in Fig. 3. It is known that an accurate estimate of k_m, and therefore D, is necessary for the determination of the active analyte concentration under conditions of partial MTL [15,16]. Given that an accurate estimate of k_m was returned from the experimental data, it was posited that the active concentration might be returned from fitting a two-compartment model.

Eq. (9) was substituted for k_m, and the TDi data in Fig. 3B were refitted solving for global values of k_a, k_d, D, and analyte

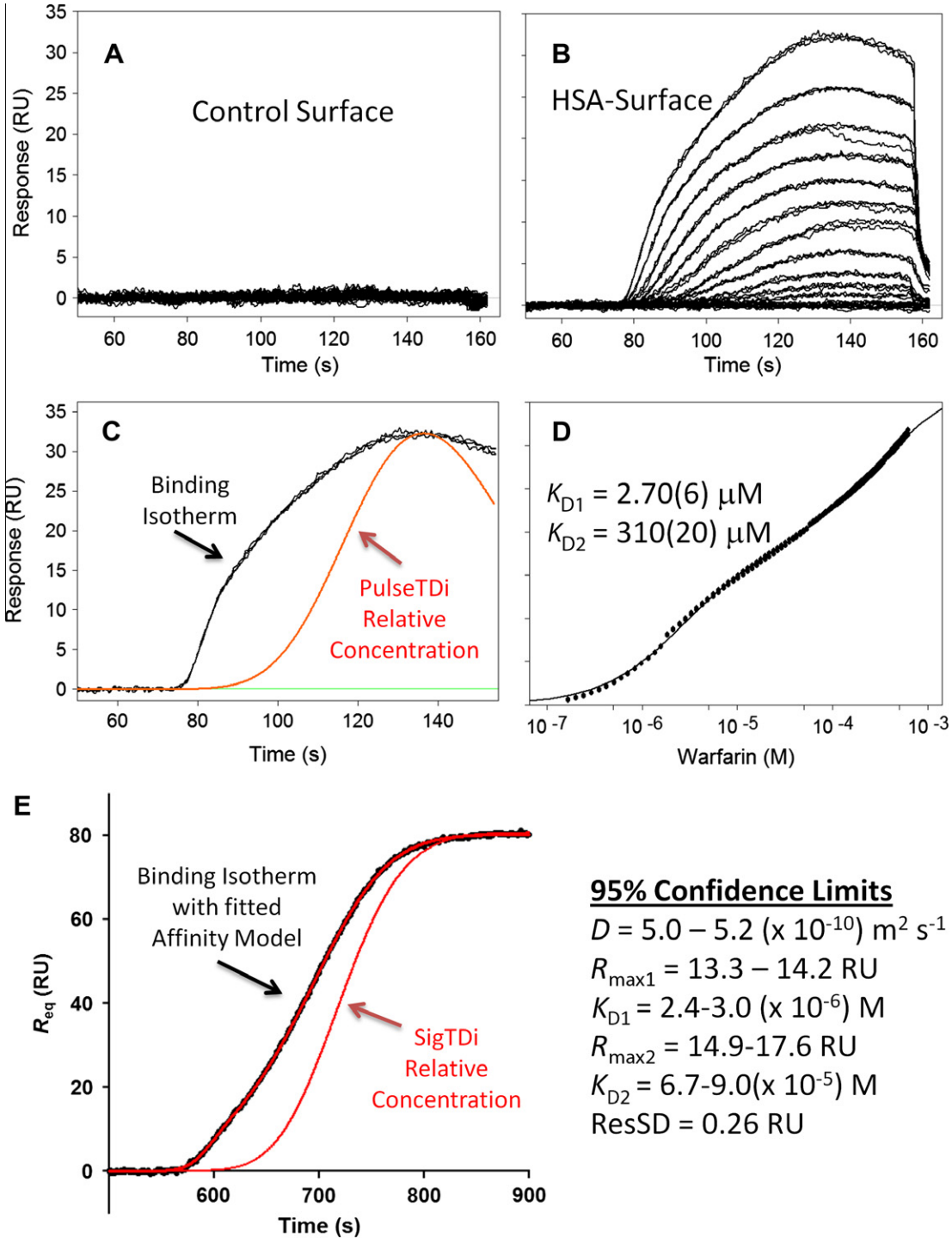

Fig.6. Affinity analyses of warfarin–HSA interaction. (A) Serial 2-fold dilutions of warfarin from 0.244 nM to 1 mM were prepared. Here, 5 µl of each was injected by PulseTDi at 25 µl min^{-1}. The superimposed double referenced response curves recorded over a noncoated sensing surface are shown for all injections. (B) Same as analysis in panel A, but the specific binding response was isolated by application of double referencing to the response curves recorded over the HSA-coated sensing surface. (C) The specific binding response curves for 1 mM warfarin were replotted together with the expected relative analyte concentration profile calculated from Eq. (1). (D) A selection of the response points from the curves in panel C were plotted with respect to the expected warfarin concentration, and a two-site steady-state affinity model was fitted using Qdat. (E) The analysis was repeated using SigTDi and a larger capillary (tube E). Here, 60 µl of 1 mM warfarin was injected by SigTDi, producing a sigmoidal dispersion. The expected relative dispersion profile is the sigmoidal (smooth red curve) curve that is shifted to the right of the experimental binding response curve (rough black curve). A three-site real-time isotherm model (Eq. (12)) was fitted using GraphPad Prism, and the fitted parameters for the two specific binding sites of interest are shown on the plot as 95% confidence limits. The fitted isotherm (smooth red curve) superimposes onto the experimental isotherm, giving an average residual SD of 0.26 RU. (For interpretation of the references to color in this figure legend, the reader is referred to the Web version of this article.)

concentration. The analyte concentration was constrained to a single global value by representing the concentrations as follows: neat, neat × 0.1, neat × 0.01, neat × 0.001, and neat × 0.0001. In practice, the analyte concentration is usually known to within 2-fold of the initial estimated value, and constraining its value within this limit ensured convergence of the model. When solving for analyte

concentration, D and k_m were held constant at 8.86×10^{-11} m^2 s^{-1} and 6.9×10^8 RU M^{-1} s^{-1}, respectively. The initial values for the fitted parameters were chosen with a high disparity with respect to the expected parameter estimates in order to provide a more realistic test of the model fit. Therefore, the initial parameter values were chosen as R_{max} = 40 RU, $k_a = 5 \times 10^4$ M^{-1} s^{-1}, $k_d = 1 \times 10^{-3}$ s^{-1}, and analyte concentration = 5×10^{-6} M.

Despite the low level of MTL, the analysis returned an accurate analyte concentration in addition to parameter values almost identical to those in Fig. 3. The returned parameters were R_{max} = 35.012(2) RU, $k_a = 6.5(2) \times 10^5$ M^{-1} s^{-1}, $k_d = 6.91(2) \times 10^{-5}$ s^{-1}, and analyte concentration = $1.01(3) \times 10^{-6}$ M. The analyte concentration was expected to be 1 μM because the k_m employed in this fit was obtained from a previous fit where the concentration was assumed to be exactly 1 μM. An insignificant change in active concentration was observed when the analysis was repeated using the expected k_m (6.82×10^8 RU M^{-1} s^{-1}). While mindful of the risk of overinterpreting the results, the accuracy and SE of the returned analyte concentration were remarkable, whereas k_a remained accurate, albeit with an increased SE.

Furosemide–carbonic anhydrase II interactions

Furosemide is a carbonic anhydrase inhibitor with an M_r of 336. Its diffusion coefficient is expected to be 5.33×10^{-10} m^2 s^{-1} from the Stokes–Einstein–Sutherland equation [11]. Kinetic analysis of furosemide binding to immobilized carbonic anhydrase II is shown in Fig. 4. A series of serial 2-fold dilutions was analyzed in triplicate by FCI, and the data were globally fitted with a 1:1 interaction model, as shown in Fig. 4A. As expected, the model interaction was well described by the simple model. The analysis was repeated by TDi using serial 10-fold dilutions, and the results for a fit to a global 1:1 interaction model are shown in Fig. 4B. Replicate TDi curves showed high reproducibility at each injected concentration, and the kinetic constants were comparable to those from FCI analysis. The TDi curves covered a concentration range of 1000-fold, whereas FCI curves covered a much lower range of 252-fold. The FCI concentrations approximate the limits that produce sufficient curvature for reliable kinetic analysis. Therefore, concentrations outside this range provide little kinetic information. In contrast, TDi curves provide adequate kinetic curvature over a wider range, being effectively unbounded at higher concentrations. The fitted parameter, D, was practically identical to the predicted value, indicating that the analyte was not aggregated. Both TDi and FCI gave reasonable SDs of the residuals for each global fit. Interestingly, the SE associated with fitting k_a to TDi data was 20-fold lower than that from FCI data, indicating higher confidence in TDi analysis.

Multisite furosemide–carbonic anhydrase II binding

To investigate resolution of two-site binding by TDi, a carbonic anhydrase II-coated sensing surface was allowed to degrade and binding of furosemide was recorded at 10 °C, as shown in Fig. 4C. Nonspecific binding became significant at higher analyte concentrations, presumably because the degraded carbonic anhydrase II presented more hydrophobic pockets than the native form of the protein. Visual inspection of the data from the degraded carbonic anhydrase II surface revealed that specific analyte binding occurred earlier for the higher affinity site, enabling the curve-fitting algorithm to readily distinguish both components. A global fit of a two-site interaction model to the TDi data resolved the kinetic constants for the specific affinity site in the presence of a larger response from the nonspecific binding site while also returning D. Low variation (CV = 3.6%) in k_a between curves was observed when each curve was fitted separately (i.e., locally), indicating that a single curve provided a reliable estimate of the kinetic constants. More significant, nonspecific binding comprising approximately 70% of the total binding response did not interfere significantly with estimation of the kinetic constants from single TDi curves. The value of D obtained from the two-site fit was within 10% of the expected value after correction for a temperature offset of 15 °C, suggesting that analyte aggregation at the lower analysis temperature was not significant.

Affinity ranking

In some applications, it is not appropriate to fit a kinetic model, and a simple means of providing a kinetic/affinity ranking can suffice. For example, many proteins degrade rapidly or shift between different conformational states [23,24], and if these changes occur while a kinetic/affinity analysis is being performed, the recorded data represent the average kinetic/affinity state during the assay. Changes in binding properties that occur within minutes can be monitored using the TDi approach, providing a detailed account of the changing binding characteristics. Using warfarin–HSA as a model, it was possible to track changes in the affinity for a two-site interaction while the HSA was in transition between different conformations. Therefore, the overlaid binding response curves in Fig. 5 effectively represent a time-series progression where dynamic changes in affinity can be qualitatively compared. Three or more binding rate peaks are visible in the derivative plot in Fig. 5 (inset plot), and the progression of these binding sites toward lower affinity (i.e., shift to right) is evident.

Real-time isotherm

TDi may provide a rapid method for affinity determination of compounds in label-free screening. The model interaction of warfarin with HSA is characteristic of fragment screen interactions, where both the M_r and affinity are low, and was employed to demonstrate the real-time isotherm technique. Typically, the approach to steady state is almost instantaneous when the affinity is low and the kinetic constants are relatively fast. Under these conditions, the TDi binding response curve can be treated as a real-time affinity isotherm. Both PulseTDi and SigTDi analyses produced equivalent results, as shown in Fig. 6. The effectiveness of double referencing is evident in Fig. 6A given the absence of any response over a control sensing surface. Therefore, we may assume that all interferences have been accurately subtracted from the warfarin–HSA curves in Fig. 6B. PulseTDi was repeated for a series of warfarin concentrations in order to demonstrate the reproducibility of the technique. Each concentration was repeated in triplicate and produced binding curves that were essentially superimposable with the exception of 1 partially outlying curve from a set of 36. The binding curves for 1 mM warfarin are shown separately in Fig. 6C along with the expected analyte dispersion profile calculated from Eq. (1), where D was calculated from the Stokes–Einstein–Sutherland equation [11]. A subset of response points were selected from these curves and plotted against the expected concentration. A two-site affinity model was fitted to this isotherm, as shown in Fig. 6D. The resulting affinity constants were in good agreement with literature values [5,6] and were also in good agreement with a replicate analysis performed by SigTDi (Fig. 6E). Eq. (12) was directly fitted to the SigTDi isotherm, which, in contrast to a standard isotherm plot (i.e. R_{eq} vs. concentration), enables D to be fitted. The 95% confidence limits for each returned parameter indicated that both high-affinity and low-affinity sites are well determined from a single TDi curve. However, when run times are less critical, it is advisable to include another SigTDi curve at a 10-fold lower concentration , or alternatively at the same concentration but at a different injection flow rate, to further improve the parameter confidence intervals. This also improves resistance to occasional

interferences that do not subtract exactly on double referencing. Other more complex binding models might benefit from application of TDi, but these are beyond the scope of the current article.

Conclusion

TDi forms highly ordered analyte gradients, without added cost in terms of complexity or expense, for enhanced resolution of both simple and complex biomolecular binding interactions. TDi enabled high-quality kinetic analysis over a broad M_r range, giving reliable estimates of the analyte diffusion coefficients in addition to the kinetic interaction constants. Kinetic analyses of single TDi curves were shown to provide parameter estimates that were as reliable as those from a global model fit to multiple standard injection curves. The presence of nonspecific binding comprising as much as 70% of the recorded binding response did not prevent resolution of the high-affinity interaction constants from single TDi curves. TDi provided reliable estimates of k_a, k_d, R_{max}, D, and active analyte concentration from a single set of binding interaction curves. A real-time isotherm that provided unprecedented resolution of multisite interactions was demonstrated and may be of particular interest in compound screening applications. Sample preparation, assay setup, and method programming were simplified in comparison with the standard approach. In conclusion, enhanced biophysical characterization was possible while reducing assay complexity and run time.

Acknowledgments

I thank Chris Strande and Tom Morton for software and thank Lena Flood for assistance with preparing the manuscript.

References

[1] D.L. Phillips, A technique for the numerical solution of certain integral equations of the first kind, J. Assist. Comput. Mach. 9 (1962) 83–97.
[2] J.M. Varah, On fitting exponentials by nonlinear least squares, Siam J. Sci. Stat. Comput. 6 (1985) 30–44.
[3] K.E.D. Coan, B.K. Shoichet, Stoichiometry and physical chemistry of promiscuous aggregate-based inhibitors, J. Am. Chem. Soc. 130 (2008) 9606–9612.
[4] A.M. Giannetti, B.D. Koch, M.F. Browner, Surface plasmon resonance based assay for the detection and characterization of promiscuous inhibitors, J. Med. Chem. 51 (2008) 574–580.
[5] R.L. Rich, Y.S.N. Day, T.A. Morton, D.G. Myszka, High-resolution and high-throughput protocols for measuring drugs/HSA interactions using BIACORE, Anal. Biochem. 296 (2001) 197–207.
[6] Y.S.N. Day, D.G. Myszka, Characterizing a drug's primary binding site on albumin, J. Pharm. Sci. 92 (2003) 333–343.
[7] A.M. Giannetti, From experimental design to validated hits: a comprehensive walk-through of fragment lead identification using surface plasmon resonance, Methods Enzymol. 493 (2011) 169–218.
[8] G. Taylor, Dispersion of soluble matter in solvent flowing slowly through a tube, Proc. R. Soc. London, A 219 (1953) 186–203.
[9] R.R. Walters, J.F. Graham, R.M. Moore, D.J. Anderson, Protein diffusion coefficient measurements by laminar flow analysis: method and applications, Anal. Biochem. 140 (1994) 190–195.
[10] V. Ananthakrishnan, W.N. Gill, A.J. Barduhn, Laminar dispersion in capillaries: I. Mathematical analysis, AIChE J. 11 (1965) 1063–1072.
[11] M.E. Young, P.A. Carroad, R.L. Bell, Estimation of diffusion coefficients of proteins, Biotechnol. Bioeng. 22 (1980) 947–955.
[12] I.N. Serdyuk, N.R. Zaccai, J. Zaccai, Methods in Molecular Biophysics: Structure, Dynamics, Function, Cambridge University Press, Cambridge, UK, 2007.
[13] D.G. Myszka, X. He, M. Dembo, T.A. Morton, B. Goldstein, Extending the range of rate constants available for BIACORE: interpreting mass transport-influenced binding data, Biophys. J. 75 (1998) 583–594.
[14] D.G. Myszka, T.A. Morton, M.L. Doyle, I.M. Chaiken, Kinetic analysis of a protein antigen–antibody interaction limited by mass transport on an optical biosensor, Biophys. Chem. 64 (1997) Z127–Z137.
[15] L.L.H. Christensen, Theoretical analysis of protein concentration determination using biosensor technology under conditions of partial mass transport limitation, Anal. Biochem. 249 (1997) 153–164.
[16] K. Sigmundsson, G. Másson, R. Rice, N. Beauchemin, B. Öbrink, Determination of active concentrations and association and dissociation rate constants of interacting biomolecules: an analytical solution to the theory for kinetic and mass transport limitations in biosensor technology and its experimental verification, Biochemistry 41 (2002) 8263–8276.
[17] D.B. Hand, The refractivity of protein solutions, J. Biol. Chem. 108 (1934) 703–707.
[18] A.R. Katritzky, S. Sild, M. Karelson, General quantitative structure–property relationship treatment of the refractive index of organic compounds, J. Chem. Inf. Comput. Sci. 38 (1998) 840–844.
[19] D.G. Myszka, Improving biosensor analysis, J. Mol. Recognit. 12 (1999) 279–284.
[20] W. M Saltzman, M.L. Radomsky, K.J. Whaley, R.A. Cone, Antibody diffusion in human cervical mucus, Biophys. J. 66 (1994) 508–515.
[21] A. Önell, K. Andersson, Kinetic determination of molecular interactions using Biacore: minimum data requirements for efficient experimental design, J. Mol. Recognit. 18 (2005) 307–317.
[22] S. Kubetzko, C.A. Sarkar, A. Plückthun, Protein PEGylation decreases observed target association rates via a dual blocking mechanism, Mol. Pharmacol. 68 (2005) 1439–1454.
[23] S.H. Scheres, H. Gao, M. Valle, G.T. Herman, P.B. Eggermont, J. Frank, J.M. Carazo, Disentangling conformational states of macromolecules in 3D–EM through likelihood optimization, Nat. Methods 4 (2007) 27–29.
[24] K. Saito, K. Hamano, M. Nakagawa, K. Yugawa, J. Muraoka, H. Kuba, K. Furukawa, T. Azuma, Conformational analysis of human serum albumin and its non-enzymatic glycation products using monoclonal antibodies, J. Biochem. 149 (2011) 569–580.